Catalysis Today 142 (2009) 215–219

Contents lists available at ScienceDirect

Catalysis Today

journal homepage: www.elsevier.com/locate/cattod

MoO_x-based catalysts for the oxidative dehydrogenation (ODH) of ethane to ethylene
Influence of vanadium and phosphorus on physicochemical and catalytic properties

N. Haddad [a], E. Bordes-Richard [b], A. Barama [a,*]

[a] Laboratoire de Chimie du Gaz Naturel, Faculté de Chimie, USTHB, BP32 El Alia, 16111 Bab Ezzouar, Alger, Algeria
[b] Unité de Catalyse et de Chimie du Solide, UMR CNRS 8181, Université des Sciences et Technologies de Lille, 59655 Villeneuve d'Ascq, France

ARTICLE INFO

Article history:
Available online 4 November 2008

Keywords:
Molybdenum oxides
Vanadium oxides
MoVPO oxides
ODH ethane

ABSTRACT

The influence of vanadium and phosphorus on the physicochemical properties of the MoO_x oxide and on its catalytic properties in the oxidation of ethane to ethylene is examined. A series of MoO_x, $MoVO_x$ (Mo/V = 11) and $MoVPO_x$ (Mo/V = 11, V/P = 1) catalysts were prepared, characterized by several techniques (BET, XRD, XPS, LRS and ATG) and studied in the oxidative dehydrogenation of ethane to ethene at atmospheric pressure and at the temperature of reaction of 550 °C. Their structural properties, during reduction and re-oxidation, were examined by in situ X-ray diffraction and by X-ray photoelectron spectroscopy after pre-treatment. The sample containing phosphorus is the most active (conversion ~14%) and selective to ethylene (SC_2H_4 = 67%). The formation of $[PMo_{11}VO_{40}]^{4-}$ is assumed during preparation, and its decomposition during calcination leads to well dispersed phosphate groups and improved interactions between Mo and V species. During the catalytic reaction Mo^{VI} is stabilised by means of solid solutions of V in Mo_5O_{14} and in MoO_3 ($V_xMo_{1-x}O_{3-x/2}$). A synergetic effect between these two phases could be responsible for the best performance of $Mo_{11}VPO_x$ as compared to those of MoO_x and $Mo_{11}VO_x$.

1. Introduction

The light olefins are intensively used as intermediates in a large number of industrial syntheses like polymerisation, and ways to produce them are still welcome. The most known processes consist in operating by dehydrogenation at high temperature or oxidative dehydrogenation ODH [1]. Many formula have been studied during the last two decades, which are either based on alkali, alkaline-earth or rare-earth metal oxides [2,3], or on transition metal oxides [4,5]. Vanadium and molybdenum-based catalysts have been extensively studied in this reaction [6–8]. Mo–V–Nb mixed oxides [9], doped with Pd [10–12], or Ca [13], supported vanadium oxide [14,15], bi-doped VPO catalysts [16], were reported to be more or less active and selective in to ethene or to acetic acid. High yields to ethene of ca. 75% were obtained by using MoVNbTe catalysts [17,18]. Previously, the Mo_5O_{14}-type phase was found to be related with good performance in the selective oxidation of ethane to acetic acid. Roussel et al. [12] proposed that a synergetic effect between nanocrystals of $(VMoNb)_5O_{14}$ and $V_xMo_{1-x}O_{3-x/2}$ is responsible for the high catalytic performance of this multicomponent MoVNb(Pd) oxide. In a former work we had examined the catalytic and structural properties of Mo-based species supported on alumina in ODH of ethane with O_2 as oxidant [19]. Here, we report on the catalytic and structural properties of unsupported molybdenum oxide catalysts modified by vanadium and phosphorus in the ODH of ethane.

2. Experimental

2.1. Preparation and characterization of catalysts

MoO_x, $MoVO_x$ (Mo/V = 11) and $MoVPO_x$ (Mo/V = 11, Mo/P = 11) solids (further noted Mo, $Mo_{11}V$ and $Mo_{11}VP$, respectively) were prepared by adding $(NH_4)_6Mo_7O_{24}{\cdot}4H_2O$, $(NH_4)_2HPO_4$ and NH_4VO_3 salts in stoichiometric amounts in aqueous solution [19]. The solid residue was dried in air at 100 °C and calcined in a flow (0.55 cm3 s^{-1}) of dry air at 400 °C for 16 h. Particles of catalyst were sieved to diameters of 180–355 μm. The catalysts were characterized and tested as described in this Ref. [19].

* Corresponding author. Tel.: +213 21 24 79 64; fax: +213 21 24 73 11.
E-mail address: a_barama@yahoo.fr (A. Barama).

0920-5861/$ – see front matter © 2008 Elsevier B.V. All rights reserved.
doi:10.1016/j.cattod.2008.09.015

In all experiments, the performances were evaluated by conversion, selectivity and yields calculated as follows:

$$C_2H_6\ \text{conv.}(\%) = \frac{\text{moles of } C_2H_6 \text{ converted} \times 100}{\text{moles of } C_2H_6 \text{ in feed}}$$

$$\text{sel. of product}(i)(\%) = \frac{\text{moles of product } (i) \times 100}{\text{moles of all formed}}$$

Yield product (i) = conv. C_2H_6 × sel. (product i).

2.2. Physicochemical analyses

The specific areas of calcined Mo, $Mo_{11}V$ and $Mo_{11}VP$ samples (2–6 m^2/g) are low. They are not affected by the catalyst composition nor catalytic test (Table 1).

The Mo, $Mo_{11}V$ and $Mo_{11}VP$ catalysts were analyzed by XRD before and after the catalytic reaction at 550 °C. All patterns of calcined samples showed the lines characteristic of orthorhombic α-MoO_3. In $Mo_{11}VP$ and $Mo_{11}V$ the lines of vanadium oxides and/or of phosphorus oxides or of phases of the V–P–O system were absent in all calcined samples (Fig. 1). After catalytic reaction α-MoO_3 is again observed in all samples. However in the case of $Mo_{11}VP$ catalyst, the lines characteristic of $V_xMo_{1-x}O_2$ ($x \leq 0.33$) solid solution (2θ ~37.8 and 54.3° besides lines assigned to MoO_2 and to the solid solution) are observed (Fig. 2).

The Raman spectra of fresh and used Mo, $Mo_{11}V$ and $Mo_{11}VP$ samples were recorded at room temperature (Figs. 3 and 4). Before reaction (Fig. 3), the spectrum is the same whichever the examined particles (except the relative intensity of lines which may be different) which means, in first approximation, that samples show the same phases but with different relative populations. All solids exhibit Raman lines at 995, 818, 667, 380, 288, 248 and 205 cm^{-1} which are characteristic of α-MoO_3 [20]. Lines occurring at 995, 705, 531, 486, 408 and 308 cm^{-1} in $Mo_{11}V$ and $Mo_{11}VP$ are assigned to bulk V_2O_5 [21]. As this oxide was not detected by XRD, its particles are smaller than 4 nm (limit detection of the XRD technique). After catalytic reaction (Fig. 4), V_2O_5 lines have disappeared from $Mo_{11}V$ and $Mo_{11}VP$ spectrum, and two additional lines appeared at 1007 and 945 cm^{-1} in the case of $Mo_{11}VP$. The line at 1007 cm^{-1} is assigned to terminal Mo = O in dehydrated Mo oxide [22]. According to Mestl [23,24] the line at 945 cm^{-1} is attributed to vibrations of Mo–O–V linkages. In their study of Mo–V–Nb–Pd–O catalysts, Roussel et al. showed that such vibrations could account for V-doped Mo_5O_{14} and hexagonal or orthorhombic molybdenum oxides containing minor amounts of vanadium (e.g. $Mo_{1-x}V_xO_{3-x/2}$, $x < 0, 2$) [12]. Thus, it may be concluded that during the catalytic reaction, Mo and V interacted thereby forming mixed Mo–O–V phases like $Mo_{1-x}V_xO_{3-x/2}$.

The binding energies (BE) of Mo*3d5/2*, V*2p3/2* and P*2p* photopeaks for catalysts calcined at 400 °C are reported in Table 2. The binding energy of Mo is 233.0 eV (Mo^{6+} in MoO_3) and the symmetry and small FWHM of the Mo signal do not allow to say that Mo^{4+} or Mo^{5+} are present in samples. On the contrary part of vanadium V^{5+} is reduced as V^{4+}. The relative amounts of V^{5+} and V^{4+} obtained after photopeak decomposition are reported in Table 2. The values of M/Mo (M = V, P) ratios were calculated for $Mo_{11}V$ and $Mo_{11}VP$ catalysts (Table 3). The theoretical formula, starting from the initial stoichiometry and considering that the oxidation state of vanadium may be (+V) or (+IV) is respectively $Mo_{11}{}^{6+}V_1{}^{5+}O_{35.5}$ – $Mo_{11}{}^{6+}V_1{}^{4+}O_{35}$ for $Mo_{11}V$, and $Mo_{11}{}^{6+}V_1{}^{5+}P_1{}^{5+}O_{38}$ – $Mo_{11}{}^{6+}V_1{}^{4+}P_1{}^{5+}O_{37.5}$ for $Mo_{11}VP$. In $Mo_{11}V$, the surface (≈100 nm depth analysis) amount of V is far lower than expected whereas it is normal in $Mo_{11}VP$. On the contrary P/Mo is higher (0.39 vs. 0.09), meaning that phosphorus is essentially localized on the $Mo_{11}VP$ surface and not in the bulk. The difference between the Mo/V ratios observed for $Mo_{11}V$ and $Mo_{11}VP$ reveals the influence of phosphorus on the surface composition. Indeed, the P addition to $Mo_{11}V$ solid results in an increase of surface vanadium (V/Mo = 0.09 for $Mo_{11}VP$ vs. 0.04 for

Table 1
Variation of the specific surface area of Mo-containing catalysts.

Catalyst	MoOx	$Mo_{11}V$	$Mo_{11}VP$
Fresh catalyst	2	5	6
Used catalyst	1	2	3

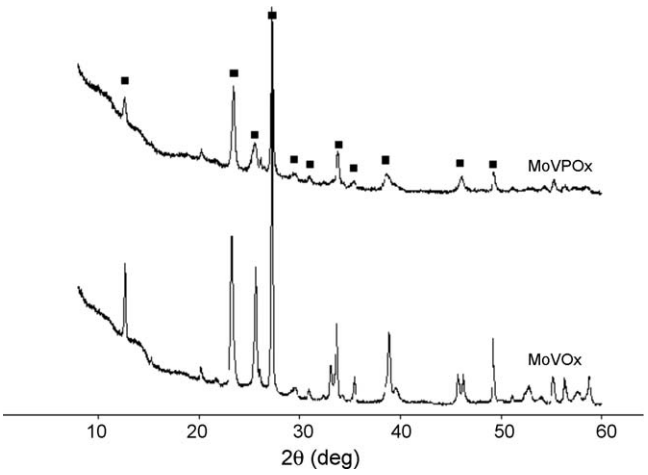

Fig. 1. XRD pattern of $Mo_{11}V$ and $Mo_{11}VP$ calcined at 400 °C; ■: MoO_3.

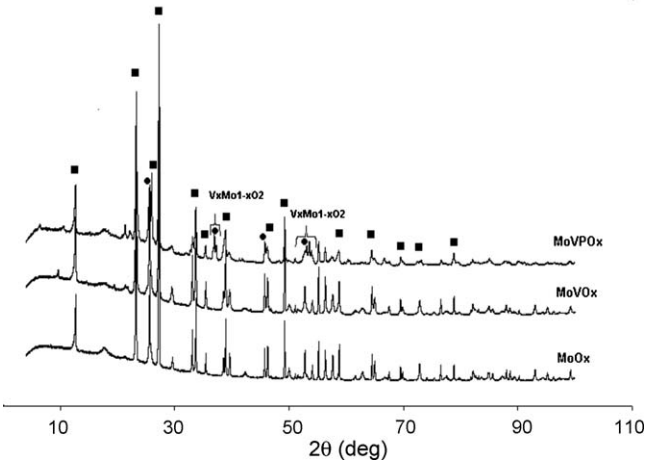

Fig. 2. XRD pattern of $Mo_{11}VP$, $Mo_{11}V$ and Mo after reaction at 550 °C; ■: MoO_3, ●: $V_xMo_{1-x}O_2$.

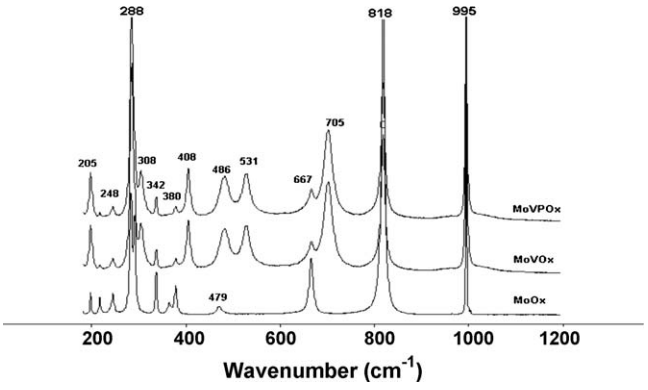

Fig. 3. Raman spectra of MoO_x, $Mo_{11}V$ and $Mo_{11}VP$ catalysts calcined at 400 °C.

Table 2
XPS results: binding energies of Mo-containing catalysts calcined at 400 °C.

BE (eV)	Mo^{6+}	V^{5+}	V^{4+}	P^{5+}	O *1s*
Mo	233.0	–	–	–	531.0
$Mo_{11}V$	232.9	517.4	516.4	–	531.0
$Mo_{11}VP$	233.0	517.4	516.4	134.3	531.0

$Mo_{11}V$), and contributes to stabilise a part of Mo in the bulk, which, otherwise, tends to diffuse towards the surface as generally observed in most Mo-based catalysts [12,25]. Possibly also, P has a slight effect on the oxidation state of V since V^{5+}/V_{tot} increases from 0.87 in $Mo_{11}V$ to 0.93 in $Mo_{11}VP$.

The structural properties of the solids during reduction by H_2/N_2 and re-oxidation by air were studied by HT-XRD in the temperature range 25–550 °C (Figs. 5–8).

Two main types of diffraction pattern are observed during reduction depending on the composition of catalyst. By heating $Mo_{11}V$ in H_2/N_2, MoO_2 characterised by lines at $2\theta = 26.0$, 37.0, 41.5, 53–54°, is formed above 500 °C, while no line of reduced vanadium oxide is observed (Fig. 5). In $Mo_{11}VP$, in addition to (V–Mo)O_2 lines (Fig. 6), new lines characteristic of Mo_5O_{14}-type structure appear at 550 °C. The presence of this phase is ascertained by the most intense diffraction at d(Å)/2θ° = 3.99/22.2 and 3.56/24.94 (JCPDS 31-1437). According to Dieterle et al. [26], the Mo_5O_{14}-type oxide crystallizes after thermal activation in a narrow temperature range between 530 and 550°. Monoclinic MoO_2 and orthorhombic V-doped MoO_3 ($Mo_{1-x}V_xO_{3-x/2}$) were additionally observed [12]. It suggests that the intermediate higher abundance of MoO_2-type oxide is related to the formation process of the crystalline Mo_5O_{14}-type material. Kihlborg reported that Mo_5O_{14} can be generated by tempering the respective amounts of MoO_2 and MoO_3 during synthesis [27]. At 550 °C the lines assigned to MoO_3 almost disappeared.

After the reoxidation step, the main phase identified in $Mo_{11}V$ above 400 °C is α-MoO_3. At this temperature, the lines of MoO_2 have completely disappeared (Fig. 7). The reoxidation of $Mo_{11}VP$ at different temperatures (Fig. 8) leads to the disproportionation of the metastable Mo_5O_{14}-type phase into the thermodynamically stable phases MoO_2 and MoO_3 or $V_xMo_{1-x}O_{3-x/2}$. This result is in agreement with Knobl et al. findings [28] who showed that the thermal treatment of doped-Mo_5O_{14} in inert atmosphere results in the formation of MoO_2, while treatment in air leads to MoO_3.

The atomic ratios and the stoichiometry, obtained from the comparison of Mo3d, V2p, O 1s and P2p photopeaks in XPS are presented for calcined, reduced and reoxidised catalysts (Table 4).

During reduction of $Mo_{11}V$ and $Mo_{11}VP$ catalysts treated at 450 °C with diluted C_2H_6, both molybdenum and vanadium are mostly reduced to Mo^{5+} and V^{4+}. The effect of the reduction step on the dispersion of Mo, V and P species is significant as shown by strong increases of V/Mo and P/Mo ratios. It means that, after reduction, Mo is slightly less present in the surface layers, or conversely that V and P are more present on the surface. In addition, the $V^{5+}/(V^{5+} + V^{4+})$ ratio decreases from 0.93 to 0.86 after calcination to 0.73–0.42 after reduction. The presence of P would decrease the reducibility of vanadium but increase the reducibility of molybdenum. Therefore, these results suggest that phosphorus is responsible for the migration of V towards surface and for partial inhibition of its reduction.

The reoxidation of reduced $Mo_{11}V$ and $Mo_{11}VP$ catalysts by O_2/N_2 led to the complete reoxidation of Mo^{5+} to Mo^{6+} and V^{4+} into V^{5+} and to the migration of more P onto the $Mo_{11}VP$ surface.

Table 3
XPS results: atomic ratios and stoichiometry of Mo-containing catalysts calcined at 400 °C.

Catalyst	Mo/V	Mo/P	V^{5+}/V_{tot}	Surface stoichiometry
$Mo_{11}V$[a]	24.4	–	0.87	$Mo_{11}\ V^{5+}_{0.39}V^{4+}_{0.06}O_{31.03}$
$Mo_{11}VP$[b]	11.0	2.55	0.93	$Mo_{11}\ V^{5+}_{0.93}V^{4+}_{0.07}P_{4.31}\ O_{40.14}$

[a] Bulk stoichiometry: between $Mo_{11}{}^{6+}V_1{}^{5+}O_{35.5}$ and $Mo_{11}{}^{6+}V_1{}^{4+}O_{35}$.
[b] Bulk stoichiometry: between $Mo_{11}{}^{6+}V_1{}^{5+}P_1{}^{5+}O_{38}$ and $Mo_{11}{}^{6+}V_1{}^{4+}P_1{}^{5+}O_{37.5}$.

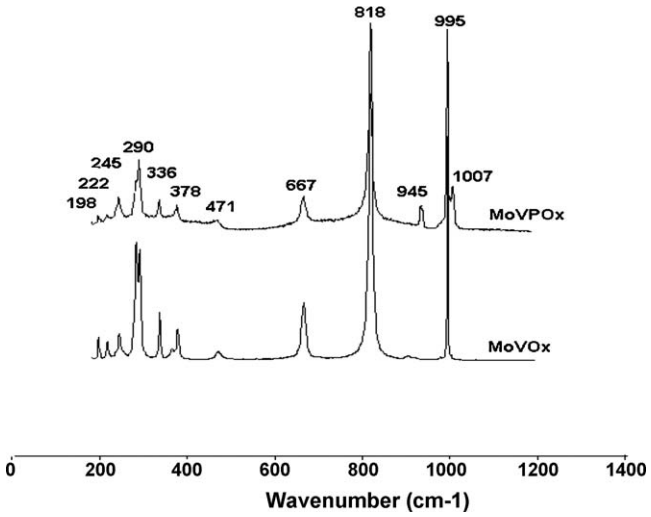

Fig. 4. Raman spectra of $Mo_{11}V$ and $Mo_{11}VP$ used catalysts.

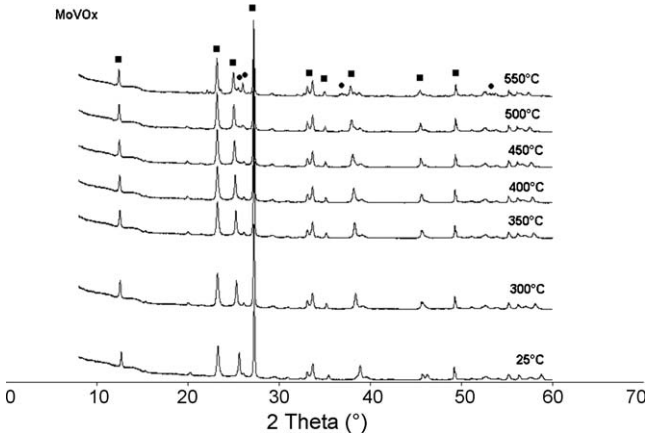

Fig. 5. XRD patterns of in situ reduction of $Mo_{11}V$ in H_2/N_2 at various temperatures (■: MoO_3, ●: MoO_2).

2.3. Catalytic properties

The catalytic activity of MoO_x, $Mo_{11}V$ and $Mo_{11}VP$ were examined in conditions of temperature, contact time and C_2H_6/O_2 such that oxygen was not fully converted. The contribution of gas-phase initiated reactions was tested by conducting experiments using an empty-volume reactor. Ethane conversion was null, confirming that gas-phase reactions are negligible under our experimental conditions.

The molybdenum-based catalysts are active in the dehydrogenation of ethane to ethylene at 550 °C and $C_2H_6/O_2 = 1$ (Table 5). The ethane and oxygen conversions increase regularly along the Mo < MoV < MoVP series. Interestingly, the selectivity to ethylene increases at the expense of the selectivity to carbon oxides. The hydrocarbon cracking represented by formation of methane

Table 4
Atomic ratios and stoichiometry of alumina-supported Mo, MoV and MoVP catalysts obtained by in situ XPS analysis after: (a), calcination at 600 °C; (b) reduction by ethane at 450 °C; (c), reoxidation by air at 450 °C.

Catalyst	V/Mo	V/P	P/Mo	V^{5+}/V_{tot}	V^{4+}/Mo	Surface stoichiometry
Mo_{11} VP						
a	0.09	0.23	0.39	0.93	0.006	$Mo_{11}V^{5+}_{0.93}V^{4+}_{0.07}P_{4.31}$ $O_{40.14}$
b	0.15	0.28	0.52	0.73	0.04	$Mo^{6+}_{8.93}$ $Mo^{5+}_{2.07}V^{5+}_{1.23}V^{4+}_{0.44}$ $P_{5.82}$ $O_{44.02}$
c	0.10	0.17	0.63	1		Mo_{11} $V^{5+}_{1.18}$ $P_{6.98}$ $O_{44.6}$
Rappt theo	0.09	1.00	0.09			
$Mo_{11}V$						
a	0.040	–	–	0.86	0.005	$Mo_{11}V^{5+}_{0.39}$ $V^{4+}_{0.06}$ $O_{31.03}$
b	0.057	–	–	0.42	0.03	$Mo^{6+}_{10.1}$ $Mo^{5+}_{0.87}$ $V^{5+}_{0.27}V^{4+}_{0.36}$ $O_{32.55}$
c	0.06	–	–	1		$Mo_{11}V^{5+}_{0.66}O_{30.6}$
Rappt theo	0.09	–	–			

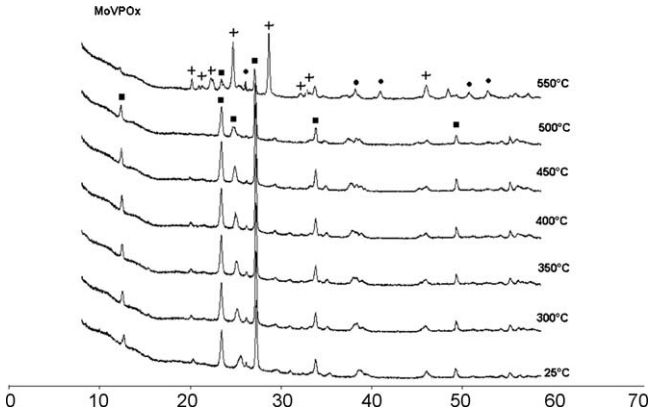

Fig. 6. XRD patterns of in situ reduction of $Mo_{11}VP$ in H_2/N_2 atmosphere at various temperatures (■: MoO_3, ●: MoO_2, +: Mo_5O_{14}).

remains very low on all catalysts. The addition of vanadium to Mo (Mo/V = 11) clearly improves both ethane conversion and selectivity to ethene, the yield of ethene increasing from 0.43 to 4.6 mol%. This improvement is even more significant in the presence of phosphorus added to $Mo_{11}V$. The 8.8 mol% yield of ethene places $Mo_{11}VP$ among the best catalysts for ODH of ethane in literature.

The enhancement of the catalytic properties of $Mo_{11}V$ upon addition of P could be related to the formation of a special active crystalline phase. Phosphorus is directly or indirectly responsible for modifications of the reactivity of both $Mo_{11}VP$ precursor and catalyst (i) during decomposition of the precursor, the stability of h-(V–Mo)O_3 oxide is improved, (ii) $Mo_{1-x}V_xO_2$ is observed by XRD in post-reaction samples, (iii) the reducibility of V^{5+} and Mo^{6+} are modified, and the relative surface amount of V is higher than for $Mo_{11}V$ (XPS), and finally (iv) $(V–Mo)_5O_{14}$ phase is formed during in situ XRD reduction. However, phosphorus as a phosphate group cannot enter these lattices without collapse of the respective structures. The only possibility would be the formation of $VOPO_4$ or related VPO (MoPO) phases, not detected by any method of analysis, but that could be present as microdomains. The chosen initial $Mo_{11}VP$ stoichiometry was expected to result in the formation of the $[PMo_{11}VO_{40}]^{4-}$ polyanion, and although the mixture was too basic to allow for the crystallisation of the ammonium salt, we assume that at the nanoscale such heteropolyanions could be present. Contrary to the case of Mo and $Mo_{11}V$ where the interaction of Mo and V is not favoured, the dispersion of vanadium and phosphorus among molybdenum species during the decomposition of $[PMo_{11}VO_{40}]$ results in an intimate mixture favouring the formation of mixed Mo–V phases and the stabilisation of Mo^{6+} species. Moreover, the precursors were deliberately calcined at a temperature (400 °C) lower than the reaction temperature (here 550 °C). The result is that, while facing the reacting mixture ethane/oxygen, the calcined solids undergo complement transformations (equilibration) as shown by the formation of $(Mo,V)_5O_{14}$. According to Banares et al. [29], such interactions are evident in used catalysts since lattice oxygen

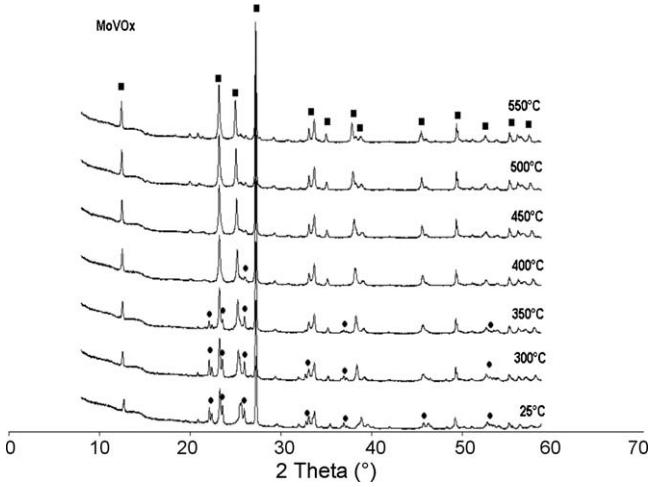

Fig. 7. XRD patterns of in situ reoxidation of $Mo_{11}V$ in O_2/N_2 atmosphere at various temperatures (■: MoO_3, ●: MoO_2).

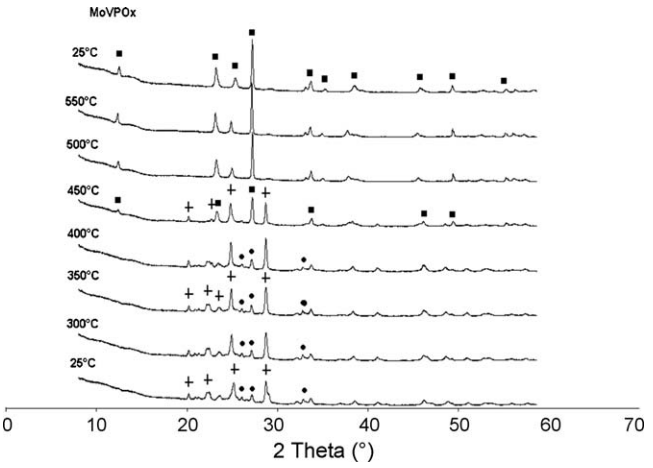

Fig. 8. XRD patterns of in situ reoxidation of $Mo_{11}VP$ in O_2/N_2 atmosphere at various temperatures (■: MoO_3, ●: MoO_2, +: Mo_5O_{14}).

Table 5
Catalytic data obtained during the oxidation of C2H6. Operating conditions: T = 550 °C, C_2H_6/O_2 = 1, τ = 0.9s.

Catalyst	C_2H_6 conv. (%)	O_2 conv. (%)	Selectivity % (yield %)		
			C_2H_4	CH_4	$CO + CO_2$
MoO_x	4.6	34.8	9.5 (0.44)	1.3	89.2
$Mo_{11}V$	8.7	49.8	52.9 (4.60)	3.6	43.5
$Mo_{11}VP$	14.3	57.6	67.7 (8.80)	1.8	30.5

mobility during the catalytic redox cycle promotes the interaction between, here, Mo and V species. Phosphate groups could also limit the size of excess MoO_3 domains, thereby stabilising them and hindering the volatility of MoO_3 (as Mo^{6+} hydrates).

From the catalytic point of view, the strong acidity of phosphate groups and of the higher amounts of vanadium present on the surface (XPS) of $Mo_{11}VP$ should influence the catalytic surface. Apart from a possible "site isolation" effect exerted on vanadium (molybdenum) sites, phosphate groups are suitable for adsorption of water which is formed besides ethene vanadium sites are more active than Mo sites because of their reducibility, and interact in a better way with ethane. The result is an increase of activity. It is worthwhile to recall that a similar behaviour has been observed with $MoVNbO_x$ system for ethane oxidation to acetic acid and ethene [11,12]. In that system, the enhancement of catalytic activity and selectivity has been related also to the presence more numerous vanadium sites, and the stabilisation of Mo^{6+} by the formation of $(V–Nb–Mo)_5O_{14}$-type microdomains. In a similar way, a synergetic effect between these structurally related oxides could be responsible for the high activity of $Mo11VPO_x$ when compared to MoO_x and $Mo11VO_x$ catalysts.

3. Conclusion

This work was devoted to the study of Mo-based catalysts differing by the nature of additive for the oxidative dehydrogenation of ethane to ethylene. Whereas MoO_x is poorly active at relatively low temperatures, its catalytic activity is enhanced when vanadium ($Mo_{11}V$) and even more when phosphorus ($Mo_{11}VP$) are added. This enhancement could be due to a different structure of the studied catalysts made up of MoO_3 particles and θ-Mo_5O_{14}-type oxide doped with a minor amount of vanadium. This surface structure would be better prepared when a $[PMo_{11}V]$ heteropoly anion is formed during synthesis because its decomposition favours further intimate interactions between Mo and V species. Equilibration on stream of the calcined catalysts also promotes such interactions. Therefore, we suggest that synergistic effects between these structurally related oxides could be responsible for the enhanced catalytic performance of $Mo_{11}VP$.

References

[1] K. Nakagawa, C. Kajita, K. Okumura, M. Na-okilkenaga, T. Nishitani-Gamo, T. Ando, T. Kobayashi, Suzuki, J. Catal. 203 (2001) 87–93.
[2] W. Ueda, S.W. Lin, I. Tohmoto, Catal. Lett. 44 (1997) 241.
[3] S. Wang, K. Murata, T. Hayakawa, S. Hamakawa, K. Suzuki, Stud. Surf. Sci. Catal. 130 (2000) 1829.
[4] Y. Schuurman, V. Ducarme, T. Chen, W. Li, C. Mirodatos, G.A. Martin, Appl. Catal. A 163 (1997) 227.
[5] F. Cavani, N. Ballarini, A. Cericola, Catal. Today 127 (1–4) (2007) 113.
[6] K. Wada, H. Yamada, Y. Watanabe, T. Mitsudo, J. Chem. Soc., Faraday Trans. 94 (1998) 1771.
[7] F.C. Meunier, A. Yasmeen, J.R.H. Ross, Catal. Today 37 (1997) 33.
[8] P. Ciambelli, P. Galli, L. Lisi, M.A. Massucci, P. Patrono, R. Pirone, G. Ruoppolo, G. Russo, Appl. Catal. A 203 (2000) 133.
[9] K. Ruth, R. Burch, R. Kieffer, J. Catal. 175 (1998) 27.
[10] D. Linke, D. Wolf, M. Baerns, O. Timpe, R. Schlögl, S. Zeyß, U. Dingerdissen, J. Catal. 205 (2002) 16, ibid., 32.
[11] M. Bouchard, M. Roussel, E. Bordes-Richard, K. Karim, S. Al-Sayari, Catal. Today 99 (2005) 77.
[12] M. Roussel, M. Bouchard, K. Karim, S. Al-Sayari, E. Bordes-Richard, Appl. Catal. A: Gen. 308 (2006) 62–74.
[13] F.G. Young, E.M. Thorsteinson, US Patent No. 4250346 (1981).
[14] B. Sulikowski, A. Kubacka, E. Wloch, Z. Schay, V. Cortés Corberan, R.X. Valenzuela, Stud. Surf. Sci. Catal. 130 (2000) 1889.
[15] D.I. Enache, E. Bordes-Richard, A. Ensuque, F. Bozon-Verduraz, Appl. Catal. A: Gen. 278 (2004) 93, ibid., 103.
[16] J.M. Lopez Nieto, V.A. Zazhigalov, B. Solsona, I.V. Bacherikova, Stud. Surf. Sci. Catal. 130 (2000) 1853.
[17] T. Katou, D. Vitry, W. Ueda, Catal. Today 91/92 (2004) 237.
[18] J.M. López-Nieto, P. Botella, P. Concepció, A. Dejoz, M.I. Vásquez, J. Catal. 209 (2005) 445.
[19] N. Haddad, E. Bordes-Richard, L. Hilaire, A. Barama, Catal. Today 126 (2007) 563.
[20] C. Stinner, R. Prins, Th. Weber, J. Catal. 191 (2000) 438.
[21] D.A. Morris, C. Kaidong, A.T. Bell, E. Iglesia, J. Catal. 208 (2002) 139.
[22] R. Iwamato, J. Grimblot, Adv. Catal., vol. 44.
[23] G. Mestl, J. Raman Spectrosc. 33 (2002) 333.
[24] G. Mestl, T.K.K. Srinivasen, Catal. Rev. Sci. Eng. 40 (1998) 451.
[25] Y.L. Leung, B.J. Flinn, P.C. Wong, K.A.R. Mitchell, K.J. Smith, Appl. Surf. Sci. 125 (1998) 293–299.
[26] M. Dieterle, G. Mestl, J. Juchida, H. Hibst, R. Schlögl, J. Mol. Catal. A: Chem. 174 (2001) 169.
[27] L. Kihlborg, Arkiv Kemi 21 (1963) 427.
[28] S. Knobl, G.A. Zenkovets, G.N. Kryukova, O. Ovsitser, D. Niemeyer, R. Schlögl, G. Mestl, J. Catal. 215 (2003) 177.
[29] M.A. Banares, S.J. Khatib, Catal. Today 96 (2004) 251.